Computational and Experimental Analysis of Pinch-Off and Scaling

Alvin U. Chen, Patrick K. Notz, and Osman A. Basaran
School of Chemical Engineering, Purdue University, West Lafayette, Indiana 47907
(Received 27 November 2001; published 12 April 2002)

Pinch-off and scaling during drop formation are studied using high-accuracy computation and ultrafast, high-resolution imaging. The interface of a water drop (viscosity $\mu \approx 1$ cP) is shown to overturn prior to breakup for the first time in experiments, well before the dynamics transitions from the potential flow (PF) to the inertial-viscous (IV) regime. A drop of 83% glycerol-water solution ($\mu \approx 85$ cP) is shown to exhibit a transition from the PF to the IV regime both computationally and experimentally. The computed value of the minimum neck radius in the latter case follows Eggers's universal solution until it becomes unstable.

DOI: 10.1103/PhysRevLett.88.174501 PACS numbers: 47.11.+j, 47.20.Dr, 47.55.Dz

Drop formation is of great practical interest because of its prevalence in applications [1,2]. Moreover, drop breakup is of great scientific interest due to the richness of the underlying physics. First, drop breakup exhibits occurrence of finite time singularities. Second, the dynamics both spatially and temporally in the vicinity of pinch-off exhibits self-similar behavior due to the large, i.e., orders of magnitude, disparity between local length and time scales and corresponding global scales. Keller and Miksis [3] first proposed a scaling theory describing the self-similar recoil of a liquid sheet upon its rupture. Since this pioneering study, a number of authors have developed scaling theories to describe rupture of liquid threads surrounded by a dynamically inactive fluid. These include rupture of a thread in which (a) inertia, viscosity, and capillarity [4], (b) inertia and capillarity [5], and (c) viscosity and capillarity [6] are important. These regimes are, respectively, referred to as inertial-viscous (IV), potential flow (PF), and viscous (V) thread regimes [7]. As a thread of a low (high) viscosity fluid initially thins according to the PF (V) scaling law, viscous (inertial) forces eventually become important so that the dynamics ultimately follows the IV scaling law so long as the effect of the outer fluid may be neglected [7].

Since self-similar behavior is observed asymptotically near pinch-off, it is of considerable scientific interest to examine through both solution of the full Navier-Stokes (NS) equations and experiment how such asymptotic states are approached. However, detailed understanding of pinch-off is not just a scientific curiosity; rupture dictates dynamics beyond pinch-off. For an algorithm that solves the NS equations—a NS solver—to remain true to physics, it must accord with scaling laws and experimental measurements made near pinch-off. This Letter presents the first combined computational and experimental study of pinch-off which uses a NS solver. Two situations are considered: (a) a low-viscosity liquid where the drop surface overturns before pinch-off, which is a challenge to both computation and experiment, and (b) a more viscous liquid where the dynamics exhibits a transition from one scaling regime to another.

The challenge to both computation and experiment in studying drop breakup is that length (time) scales may range between cm (s) and μm (μs). To date, most computations capable of accurate description of pinch-off have relied on approximations to the NS equations. These have modeled the dynamics by one-dimensional (1D), slender-jet analysis [8,9] (see [6] and [10] for other derivations of 1D equations), boundary element (BE) analysis of inviscid, irrotational flow [5], and BE analysis of Stokes flow [7]. Yildirim and Basaran [11] have used 1D equations to demonstrate change of scaling. Notz *et al.* [12] have used a NS solver to show, albeit without experimental verification, change of scaling as pinch-off nears.

Experimental studies of pinch-off are also challenging owing to the need to resolve small length and short time scales. To study dynamics of fine features such as microthreads, Henderson *et al.* [13] have used a camera capable of interframe times of 83 μs, exposure times of 10 μs, and spatial resolutions of 15.5 μm/pixel and Kowalewski [14] has used a camera capable of interframe times of 5.5 μs, exposure times of 200 ns, and spatial resolutions of 2.9 μm/pixel. Change of scaling has only been demonstrated experimentally by Rothert *et al.* [15], who have shown transition from the V to the IV regime.

In this Letter, the formation of an incompressible Newtonian liquid from a tube at constant flowrate Q is analyzed computationally by solving the NS equations using the Galerkin/finite element method (G/FEM) [12,16] with elliptic mesh generation [12,17]. The NS equations are nondimensionalized using tube radius R and capillary time $t_c = \sqrt{\rho R^3/\sigma}$, where ρ is density and σ is surface tension, as characteristic length and time scales. Using these scales, the following dimensionless groups arise: Ohnesorge number $Oh = \mu/\sqrt{\rho R \sigma}$, where μ is viscosity; Bond number $G = \rho g R^2/\sigma$, where g is the gravitational acceleration; and Weber number $We = \rho Q^2/(\pi^2 \sigma R^3)$. As shown in [7], dynamics of the outer fluid can be neglected until the dimensionless minimum radius of the thinning neck $h_{\min} \sim mOh^2$, where m is the ratio of the viscosity of the outer fluid to that of the drop.

In the experiments, images are obtained using a Cordin 220-8 imager that can capture up to 10^8 frames/s and is coupled to a Questar QM100 lens. Liquid is fed by a syringe pump to a tube of $R = 0.36$ cm whose outlet is sharpened to ensure a fixed contact line. Recording of images is triggered when a growing drop interrupts a laser beam. The liquids used are water with $\rho = 0.997$ g/cm^3, $\mu = 0.913$ cp, and $\sigma = 70.6$ dyn/cm, and a solution of 83 wt% glycerol in water (henceforward referred to as 83% glycerol) with $\rho = 1.21$ g/cm^3, $\mu = 85.4$ cp, and $\sigma = 63.1$ dyn/cm. The values of the dimensionless groups for water are $Oh = 1.81 \times 10^{-3}$, $G = 1.80$, and $We = 1.36 \times 10^{-6}$ and those for 83% glycerol are $Oh = 1.63 \times 10^{-1}$, $G = 2.45$, and $We = 4.61 \times 10^{-7}$. Spatial resolution in the images to be reported are 1.7 μm/pixel, interframe times are 5–100 μs, and exposure times are 200 ns.

Figure 1(a) shows the computed global shape and Fig. 1(b) shows a blowup of the same shape in the vicinity of $h_{\min}$ for a water drop at the incipience of pinch-off. The computed global and zoomed-in views of an 83% glycerol drop at the incipience of pinch-off are shown in Figs. 1(c) and 1(d). Computations reported have been made using 4809 mesh points along the drop surface and 350 000 unknowns, and therefore involve an order of magnitude finer resolution than those of Wilkes *et al.* [16]. Predictions of global quantities such as limiting lengths and volumes of drops at breakup by the NS solver used here are within 1% of experimental measurements and previous G/FEM computations [16]. Demonstrating the accuracy of the present NS solver in predicting local dynamics is a major goal of this paper.

Figure 1(b) shows that the computed shape of the water drop is highly overturned prior to pinch-off. Overturning in the presence of viscosity has only been shown computationally in [16] during drop formation and experimentally in [18] during rupture of a soap film. Figure 2(a) shows the computed profile of a water drop overlaid on an experimental image when the interface has just begun to overturn and demonstrates the excellent agreement between computations and experiments. The excellent agreement between the two persists to pinch-off. Figure 2(b) shows a view of the water drop at a later time than that in Fig. 2(a) and makes plain for the first time that the interface is overturned in the experiments. Overturning cannot be predicted by 1D models.

The blowup of the computed profile of an 83% glycerol drop depicted in Fig. 1(d) clearly shows the formation of a microthread from the primary thread, in accord with previous experiments [9,13,14]. Figure 2(c) shows the computed profile of this drop overlaid on an experimental image when $h_{\min} = 7.6 \times 10^{-3}$. Once again, the agreement between computations and experiments is excellent. Figure 2(d) shows a close-up experimental image of the microthread a few μs prior to rupture when its radius is on the order of 1–2 μm.

Further quantitative comparisons between computations, experiments, and scaling theories can be made by (a) examining the variation of $h_{\min}$ with time to breakup $\tau = t_b - t$, where t is time and t_b is the breakup time, and (b) demonstrating the collapse of appropriately scaled drop profiles, viz. $h(z, t)$ where h is the interface shape function and z is the axial coordinate, onto similarity solutions [4–6]. Figure 3 shows the variation of computed and experimentally measured values of $h_{\min}$ with τ for water. Since $Oh \ll 1$ in this situation, it is expected that the dynamics would follow PF scaling theory, where $h_{\min} \sim \tau^{2/3}$, once $h_{\min}$ becomes sufficiently small

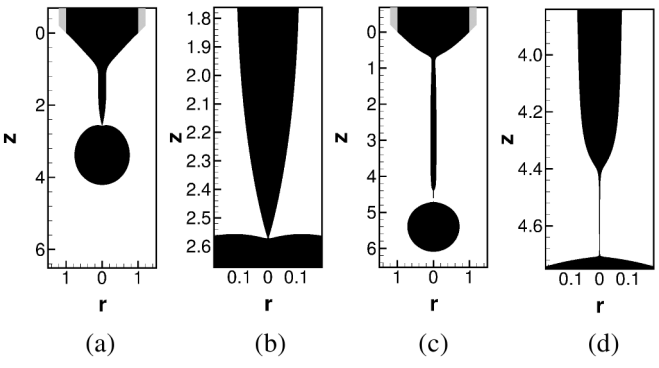

FIG. 1. Computed shapes of water, (a),(b), and 83% glycerol, (c),(d), drops at the incipience of pinch-off. Here (a) and (c) show the global shapes and (b) and (d) show their blowups in the vicinity of $h_{\min}$. For the water drop, $h_{\min} = 2 \times 10^{-3}$, and for the 83% glycerol drop, $h_{\min} = 1 \times 10^{-3}$.

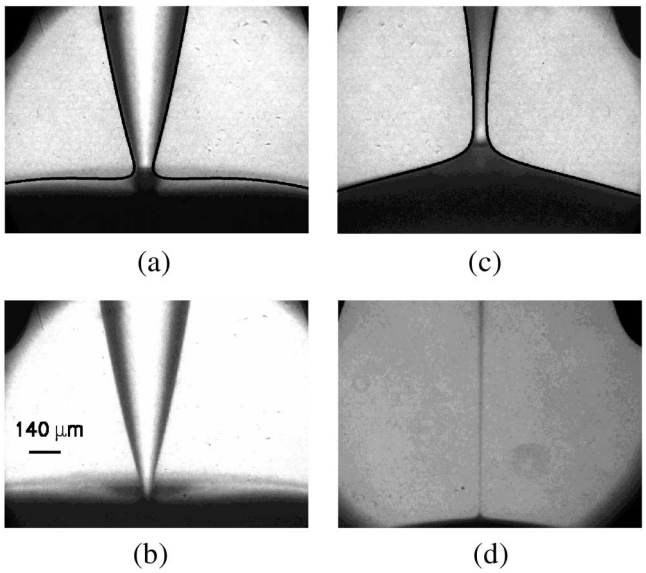

FIG. 2. (a) Computed profile of a water drop, dark curve, overlaid on an experimental image when $h_{\min} = 1.2 \times 10^{-2}$ (43 μm). (b) Experimental image of the same water drop a short time later showing a highly overturned interface. (c) Computed profile of an 83% glycerol drop, dark curve, overlaid on an experimental image when $h_{\min} = 7.6 \times 10^{-3}$ (27 μm). (d) Experimental image of the same 83% glycerol drop a short time later when the thickness of the microthread is a few μm. The scale bar shown in (b) applies to (a)–(d).

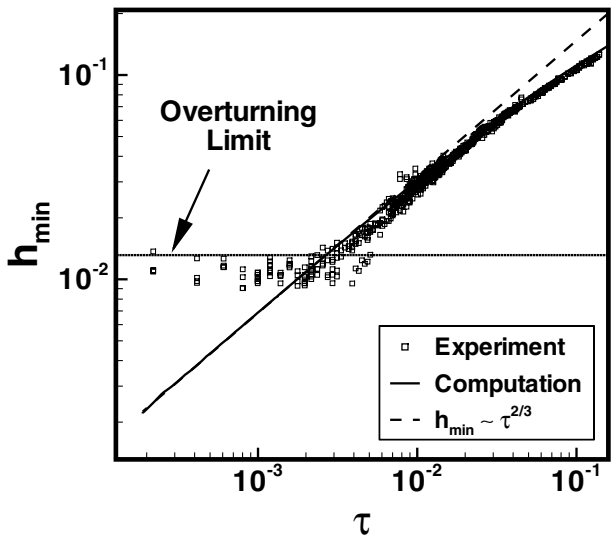

FIG. 3. Variation of computed and experimentally measured values of h_{min} with τ for water. Also shown are the PF scaling law, $h_{min} \sim \tau^{2/3}$, and the value of h_{min} when the interface overturns (overturning limit).

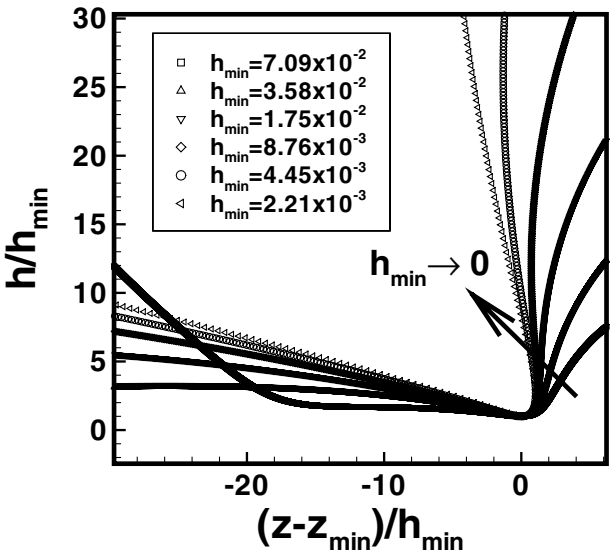

FIG. 4. Variation of computed scaled drop profiles h/h_{min} with scaled axial coordinate $(z - z_{min})/h_{min}$ for the water drop as it approaches pinch-off and the scaled shapes tend to the PF similarity solution.

[7]. Figure 3 shows that this is indeed the case when $h_{min} \approx 2 \times 10^{-2}$. Figure 3 also shows that shortly thereafter, when $h_{min} \approx 1.3 \times 10^{-2}$, the interface of the drop overturns. Once h_{min} falls below 10^{-2} (36 μm), it becomes difficult to acquire experimental data due to overturning. However, Fig. 3 shows that the computations coincide with the PF scaling result even for values of h_{min} as small as 10^{-3}. Figure 3 shows that experimental measurements and computational predictions are in excellent agreement until the overturning limit.

Figure 4 shows the variation of computed scaled drop profiles h/h_{min} as a function of scaled axial coordinate $(z - z_{min})/h_{min}$, where z_{min} is the axial coordinate where $h = h_{min}$, for the water drop as it is breaking. This figure makes plain that the scaled profiles indeed exhibit self-similarity and that the extent of the spatial coordinates over which the scaled computed solutions collapse onto the similarity solution increases as the neck thins.

The results depicted in Figs. 3 and 4 show that self-similarity and scaling as per PF scaling theory are still observed for values of h_{min} an order of magnitude smaller than that at the onset of overturning, viz. $h_{min} \approx 1.3 \times 10^{-2}$. Such results have important ramifications for analyses of breakup carried out by 1D algorithms. Indeed, the present results may at last explain the surprising breakdown of scaling reported in [19]. The transition from PF to IV scaling is expected to occur when $h_{min} \sim Oh^2$ [7]. For the water drop considered here, the transition from PF to IV scaling would occur when $h_{min} \sim 3.3 \times 10^{-6}$ (12 nm) and the dynamics of the outer fluid would come into play once $h_{min} \sim 3.3 \times 10^{-9}$.

Figure 5 shows the variation of computed and experimentally measured values of h_{min} with τ for 83% glycerol. Figure 5 shows that the dynamics initially follows PF scaling theory, a finding that accords with intuition because $Oh < 1$. Further, Fig. 5 shows that as h_{min} continues to decrease, the dynamics transitions to the IV regime, where $h_{min} \sim \tau$ [4]. Figure 5 highlights that computations and experiments are in excellent agreement with each other over roughly 2 orders of magnitude in h_{min} and that this is the first time that transition in scaling from the PF to the IV regime has been shown experimentally. As h_{min} continues to decrease, Fig. 5 shows that the computed thinning of the neck follows Eggers's universal solution

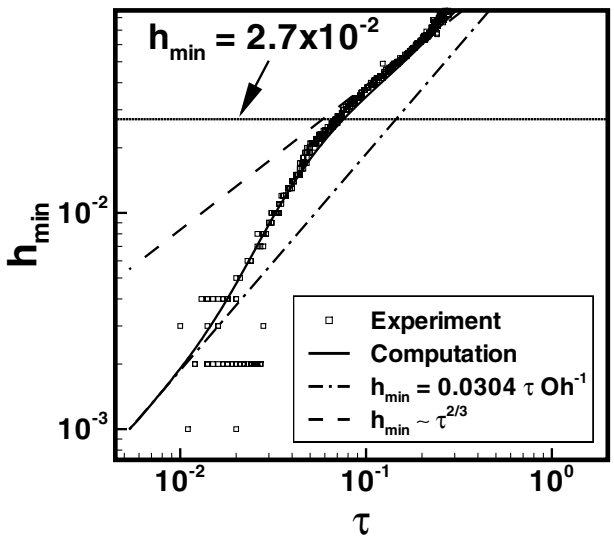

FIG. 5. Variation of computed and experimentally measured values of h_{min} with τ for 83% glycerol. For large τ, both follow the PF scaling law, $h_{min} \sim \tau^{2/3}$, and then transition to the IV scaling regime where Eggers's universal solution, $h_{min} = 0.0304\tau Oh^{-1}$, holds. The horizontal line shows when h_{min} equals the dimensionless viscous length or Oh^2.

for which $h_{\min} = 0.0304\tau Oh^{-1}$. By this time thread radius has become too small to measure experimentally and one must rely on computations to confirm Eggers's solution. As in Fig. 4, one can plot (not shown) the variation of computed scaled drop profiles $h/h_{\min}$ as a function of scaled axial coordinate $(z - z_{\min})/h_{\min}$ for the 83% glycerol drop as the neck thins but $h_{\min}$ remains large enough that Eggers's universal solution is not observed. Such a plot shows that the shapes are self-similar only over a short time $\sim 1.2 \times 10^{-2} < h_{\min} < \sim 2.5 \times 10^{-2}$ and then move away from the PF similarity solution as viscous effects become locally important, in accord with results showing change of scaling from the PF to the IV regime in Fig. 5. Figure 6 shows the variation of computed scaled drop profiles $h/h_{\min}$ as a function of scaled axial coordinate $(z - z_{\min})\tau^{1/2}/h_{\min}$ for the 83% glycerol drop as it approaches pinch-off. This figure shows that the scaled profiles exhibit self-similarity as $h_{\min}$, $\tau \rightarrow 0$ and approach Eggers's asymmetric, self-similar profile for an IV thread. Calculations have been made for values of $h_{\min}$ smaller than those shown in Figs. 5 and 6. They reveal that Eggers's universal solution becomes unstable as blobs form on the surface of the microthread, in accord with previous works [4,19–21]. For 83% glycerol, the transition from the PF to the IV regime is expected to occur when $h_{\min} \sim 2.7 \times 10^{-2}$ (96 μm) and the dynamics of the outer fluid would come into play once $h_{\min} \sim 3.1 \times 10^{-7}$.

The results of this Letter show that the new NS solver has unprecedented accuracy: its predictions accord with both experiments and scaling theories over length scales ranging from cm to μm. NS solvers of others that use the G/FEM method have failed to show overturning [22]. NS solvers that are designed for a rougher description of complicated free surface flows [23,24] would not be able to capture details presented here. Computations are shown to provide valuable insights into phenomena when experiments are no longer useful. They reveal that there is no breakdown of scaling [19] even after the interface of a water drop overturns. Computations with the NS solver also show that Eggers's universal solution can be observed, at least in a transitional manner, in certain situations. Given the accuracy of the NS solver, it can be used with confidence in situations where the state of understanding from scaling theories and experiments may be incomplete as in liquid-liquid pinch-off [7,25].

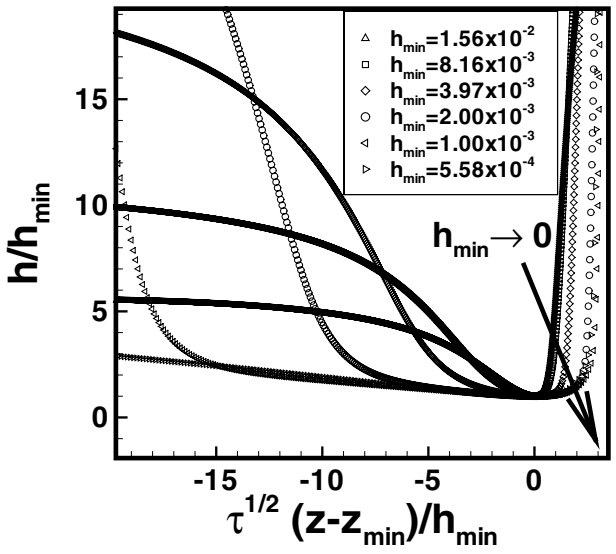

FIG. 6. Variation of computed scaled drop profiles $h/h_{\min}$ as a function of scaled axial coordinate $(z - z_{\min})\tau^{1/2}/h_{\min}$ for the 83% glycerol drop as it approaches pinch-off and the scaled shapes tend to the IV similarity solution.

This research was supported by the BES program of the U.S. DOE.

[1] H. P. Le, J. Imaging Sci. Technol. **42**, 49 (1998).
[2] W. J. Heideger and M. W. Wright, AIChE. J. **32**, 1372 (1986).
[3] J. B. Keller and M. J. Miksis, SIAM J. Appl. Math. **43**, 268 (1983).
[4] J. Eggers, Phys. Rev. Lett. **71**, 3458 (1993).
[5] R. F. Day, E. J. Hinch, and J. R. Lister, Phys. Rev. Lett. **80**, 704 (1998).
[6] D. T. Papageorgiou, Phys. Fluids **7**, 1529 (1995).
[7] J. R. Lister and H. A. Stone, Phys. Fluids **10**, 2758 (1998).
[8] J. Eggers and T. F. Dupont, J. Fluid Mech. **262**, 205 (1994).
[9] X. D. Shi, M. P. Brenner, and S. R. Nagel, Science **265**, 219 (1994).
[10] S. E. Bechtel, J. Z. Cao, and M. G. Forest, J. Non-Newtonian Fluid Mech. **41**, 201 (1992).
[11] O. E. Yildirim and O. A. Basaran, Chem. Eng. Sci. **56**, 211 (2001).
[12] P. K. Notz, A. U. Chen, and O. A. Basaran, Phys. Fluids **13**, 549 (2001).
[13] D. M. Henderson, W. G. Pritchard, and L. B. Smolka, Phys. Fluids **9**, 3188 (1997).
[14] T. A. Kowalewski, Fluid Dyn. Res. **17**, 121 (1996).
[15] A. Rothert, R. Richter, and I. Rehberg, Phys. Rev. Lett. **87**, 084501 (2001).
[16] E. D. Wilkes, S. D. Philips, and O. A. Basaran, Phys. Fluids **11**, 3577 (1999).
[17] K. N. Christodoulou and L. E. Scriven, J. Comp. Phys. **99**, 39 (1992).
[18] N. D. Robinson and P. H. Steen, J. Colloid Interface Sci. **241**, 448 (2001).
[19] M. P. Brenner, J. Eggers, K. Joseph, S. R. Nagel, and X. D. Shi, Phys. Fluids **9**, 1573 (1997).
[20] M. P. Brenner, J. R. Lister, and H. A. Stone, Phys. Fluids **8**, 2827 (1996).
[21] M. P. Brenner, X. D. Shi, and S. R. Nagel, Phys. Rev. Lett. **73**, 3391 (1994).
[22] N. Ashgriz and F. Mashayek, J. Fluid Mech. **291**, 163 (1995).
[23] M. Sussman and E. G. Puckett, J. Comput. Phys. **162**, 301 (2000).
[24] D. Gueyffier, J. Li, A. Nadim, R. Scardovelli, and S. Zaleski, J. Comput. Phys. **152**, 423 (1999).
[25] I. Cohen and S. R. Nagel, Phys. Fluids **13**, 3533 (2001).